Experimental and theoretical study on a novel double evaporating temperature chiller applied in THICS using R32/R236fa

Liu, Jian; She, Xiaohui; Zhang, Xiaosong; Cong, Lin; Man, Liang; Lindeman, Brett; Lin, Tao

[Link to publication on Research at Birmingham portal](#)

Accepted Manuscript

Title: Experimental and theoretical study on a novel double evaporating temperature chiller applied in THICS using R32/R236fa

Author: Jian Liu, Xiaohui She, Xiaosong Zhang, Lin Cong, Liang Man, Brett Lindeman, Tao Lin

Please cite this article as: Jian Liu, Xiaohui She, Xiaosong Zhang, Lin Cong, Liang Man, Brett Lindeman, Tao Lin, Experimental and theoretical study on a novel double evaporating temperature chiller applied in THICS using R32/R236fa, *International Journal of Refrigeration* (2016), http://dx.doi.org/doi: 10.1016/j.ijrefrig.2016.08.015.

Experimental and theoretical study on a novel double evaporating temperature chiller applied in THICS using R32/R236fa

Jian Liu [a], Xiaohui She [a], Xiaosong Zhang [a,*], Lin Cong [b], Liang Man [a], Brett Lindeman [c], Tao Lin [a]

[a] *School of Energy and Environment, Southeast University, Nanjing 210096, China*

[b] *School of Chemical Engineering, University of Birmingham, Birmingham, B15 2TT, UK*

[c] *Department of Mechanical Engineering, University of Wisconsin-Madison, Madison, 53706, USA*

*Corresponding author: Xiaosong Zhang, PhD.

Email: rachpe@seu.edu.cn

Highlights

- A novel double temperature chiller with zeotropic refrigerant is proposed.

- This chiller can produce chilled water with two different temperatures for THICS.

- Effect of refrigerant mass fraction on COP and second law efficiency is studied.

- Effect of water flow rate and temperature on chiller performance is studied.

Abstract

A novel chiller with double evaporating temperatures is proposed in this paper, which can be applied in temperature and humidity independent control system (THICS). A zeotropic mixture R32/R236fa is selected as the refrigerant, and chilled water with two different temperatures is produced. The experimental coefficient of performance (COP_{exp}), theoretical coefficient of performance (COP_{th}), and second law efficiency (η) of the chiller are studied. The performance of the chiller is studied by varying the mass fraction of R32 in the R32/R236fa (W(R32)), chilled water temperature, and the flow rates of the heat transfer media (chilled water and cooling water). The results show that the high temperature chilled water ($T_{H,out}$) can be at 15-18 °C, and the low temperature chilled water ($T_{L,out}$) can be at 6-8 °C. When $T_{H,out}$ is 17 °C and $T_{L,out}$ is 7 °C, the maximum COP_{th} and COP_{exp} are 4.73 and 3.97, respectively. Second law efficiency, η, increases to 31% as W(R32) increases from 0.3 to 0.6.

Keyword: double evaporating temperature; zeotropic refrigerant; second law efficiency; COP; chiller;

1

Nomenclatures

COP	coefficient of performance
C_p	specific heat capacity (kJ kg^{-1} K^{-1})
G	heat transfer media flow rate (kg s^{-1})
GTD	gliding temperature difference(^{o}C)
GWP	global warming potential
h	enthalpy (kJ kg^{-1})
$\dot{m}$	mass flow rate of refrigerant (kg s^{-1})
N	power consumption (kW)
NBP	normal boiling point (^{o}C)
ODP	ozone depression potential
P	pressure (Pa)
P_c	critical pressure (Pa)
Q	refrigerating capacity (kW)
S	entropy (kJ K^{-1})
T	temperature (^{o}C)
T_c	critical temperature (^{o}C)
W(R32)	mass fraction of R32 in mixture R32/R236fa

Greek symbol

Δ	difference
ε	relative error
η	second law efficiency

2

ξ	isentropic efficiency

Subscripts

b	bubble point temperature
com	compressor
cw	cooling water
d	dew point
eva	evaporator
exp	experiment
H	high temperature chilled water
in	inlet
L	low temperature chilled water
lo	lorenz
out	outlet
r	refrigerant
suc	suction
th	theoretical

1. Introduction

With the development of China's economy and society, the amount of energy consumed by buildings, as a percent of the total energy consumed nationally, is increasing rapidly; air conditioning is one of the main energy consumers (Cai et al., 2009). Therefore, energy conservation in air conditioning systems plays an important role in reducing the energy consumption of China.

In southern China, air humidity is very high in summer, and the humidity load takes up 50% of the cooling load

3

(Jiang, 2005). Many scholars put forward the temperature and humidity independent control system (THICS) (Wang et al., 2013; Liu et al., 2013), which separately controls air temperature and humidity, and can avoid the irreversible losses of the traditional air conditioning system (Waugaman et al., 1993; Zhao et al., 1994). In addition, it is hard for the traditional air conditioning system to meet the requirements of air temperature and humidity simultaneously (Zhao et al., 2011). At present, THICS usually uses liquid and solid desiccants to remove the latent heat and chilled water to remove the sensible heat (Ge et al., 2011; Kessling et al., 1998). Zhang (2011) proposed an operation strategy of THICS and analyzed the performance of the key components, which indicated that THICS can save 20%-30% of the consumed energy, when compared with the conventional air conditioning system. Zhao et al. (2011) tested the performance of THICS, and analyzed its yearly energy consumption. The research results showed that THICS had a significant potential for energy savings. Liquid desiccant dehumidification systems, however, have some problems such as the corrosion of pipelines and the low efficiency, which limit its applications (Lowenstein et al., 2006). There are many problems for solid desiccant dehumidification as well, such as the significant spatial requirements for the equipment and large amount of adsorbent, which increases the initial costs. In addition, solid desiccant regeneration calls for a high-grade heat source. For example, the regeneration temperature of silica gel is usually expected to be above 100 °C for practical application (Yang et al., 2012).

The *L-M* cycle was proposed by Lorenz and Meutzner (1975). The *L-M* cycle uses a zeotropic refrigerant mixture as the working fluid, which has an appropriate gliding temperature difference (*GTD*) during the evaporating and condensing processes. The energy saving potential of the *L-M* cycle was evaluated by several researchers: Lorenzand Meutzner (1975) experimentally observed 20% energy savings compared to the R12 system when an R12/R11 mixture was used; Jung (1991) reported that the *COP* increased significantly, by 15%-18%, with mixtures of R22/R123 and R32/R141b; and Zerwekh et al. (2012) and Yoon et al. (2012) showed that the energy consumption of the optimized *L-M* cycle using R290/R600(40%:60%) was 11.2% lower than that of a bypass

4

two-circuit cycle using R600a.

By taking advantage of the *L-M* cycle, a novel chiller, using R32/R236fa as the refrigerant, is presented in this paper. This chiller can provide two kinds of chilled water with different temperatures; namely, the high temperature chilled water at 17 °C and the low temperature chilled water at 7 °C. These chilled water lines can be used to handle the indoor sensible heat load and latent heat load, respectively (i.e., THICS). Both theoretical and experimental investigations are conducted in this paper. Performance of the chiller is measured as a function of the following variables: the mass fraction of R32 in mixture R32/R236fa (*W*(R32)), the chilled water temperature, and the flow rates of heat transfer media (chilled water and cooling water). This work can provide a database for the application of this chiller.

2. Theoretical analysis

2.1. Introduction of the theoretical system

A schematic of the theoretical cycle is shown in Fig. 1, which is composed of a compressor, a condenser, an expansion valve and two evaporators. In this system, later referred to as a chiller, the refrigerant entering the compressor is denoted by point 1. The state of the fluid after compression and before the condenser is point 2. After rejecting heat in the condenser, the refrigerant reaches point 3, which is just prior to the expansion valve. In the expansion valve, the refrigerant mixture is throttled, after which it reaches point 4. Between points 4 and 5, the refrigerant evaporates inside the low temperature evaporator and produces low-temperature chilled water. Following point 5, the fluid moves through the high temperature evaporator and evaporates again, producing high-temperature chilled water. This completes the system and returns the fluid to point 1, the inlet of the compressor. Fig. 2 shows the *T-S* diagram corresponding to the points in Fig. 1.

Based on REFPROP 8.0, some basic properties of the refrigerants (R32 and R236fa) are presented in Table 1. Table 2 shows the properties of the mixture R32/R236fa with different mass fraction of R32 (*W*(R32)), consisting of

5

molar mass, *NBP* (normal boiling point), critical temperature, critical pressure, *ODP* (ozone depletion potential), *GWP* (global warming potential), the latent heat capacity, and the temperature glide. It demonstrates that the *ODP* of the refrigerant mixture is zero. In addition, the refrigerant mixture has a large temperature glide, with the minimum temperature glide of 14.5 °C, which means that the chiller can meet the demands of THICS.

2.2. System performance calculation

In order to calculate the theoretical performance of the proposed chiller, the following assumptions are made:

(1) Pressure losses and the heat losses are neglected.

(2) The refrigerant leaving the condenser and high temperature evaporator is in a saturated state.

(3) The isentropic efficiency (ξ) of the compressor is assumed to be 0.7.

(4) The temperature difference during heat transfer in the condenser and evaporators is 5 °C.

The theoretical refrigerating capacity (Q_{th}), power consumption of the compressor (N_{th}) and theoretical performance (COP_{th}) are calculated in the following equations,

$$Q_{th} = \dot{m}_r (h_1 - h_4) \tag{1}$$

$$N_{th} = \dot{m}_r (h_2 - h_1) = \frac{\dot{m}_r (h_{2s} - h_1)}{\xi} \tag{2}$$

$$COP_{th} = \frac{Q_{th}}{N_{th}} \tag{3}$$

Where $\dot{m}_r$ is the mass flow rate of refrigerant.

To further analyze the proposed chiller, the ideal Lorenz cycle is studied, which consists of two isentropic processes and two isobaric processes, as shown in Fig. 3. The whole cycle can be divided into two Lorenz cycles: cycle 1-2-7-6-1 and cycle 5-7-3-4-5. In the ideal Lorenz cycle, the temperature difference between the refrigerants and the heat sources (chilled water and cooling water) is zero. In addition, the inlet temperature of the chilled water in the low temperature evaporator ($T_{L,in}$) is usually lower than the outlet temperature of chilled water in the high temperature evaporator ($T_{H,out}$). Therefore, there is a temperature jump between point 5 and point 6.

6

The evaporating temperature is assumed to be the average of the inlet and outlet temperatures of the chilled water, and the condensing temperature is regarded as the average of inlet and outlet temperatures of cooling water.

The *COP* of the Lorenz cycle can be calculated using Equation (4).

$$COP_{lo} = \frac{(T_4 + T_5)\Delta S_{4'-5'} + (T_1 + T_6)\Delta S_{5'-1'}}{((T_3 + T_7) - (T_4 + T_5))\Delta S_{4'-5'} + ((T_2 + T_7) - (T_1 + T_6))\Delta S_{5'-1'}} \tag{4}$$

In the experiment, the temperature difference of the chilled water, between the inlet and outlet of the evaporator, is controlled around 5 ^{o}C (i.e., T_5-T_4=T_1-T_6). Therefore,

$$\Delta S_{4'-5'} = \Delta S_{5'-1'} \tag{5}$$

$$T_7 = \frac{T_2 + T_3}{2} \tag{6}$$

The *COP* of the Lorenz cycle can be simplified as

$$COP_{lo} = \frac{T_4 + T_5 + T_1 + T_6}{2(T_2 + T_3) - (T_4 + T_5 + T_1 + T_6)} \tag{7}$$

3. Experimental analysis

3.1. Test apparatus

A schematic of the experimental setup is shown in Fig. 4. The chiller includes four loops: the refrigerant loop, the cooling water loop and two chilled water loops. The refrigerant loop consists of a compressor (1), a condenser (2), a reservoir (3), an expansion valve (4), a low temperature evaporator (5), and a high temperature evaporator (6). The cooling water loop and chilled water loop have the same components, which include a water pump (7), an electrical heater (8), a flow meter (9), a water tank (10), and a valve (11).

The compressor is a hermetically-sealed rotary compressor with a rated power of 1.1 kW. The condenser is a double-pipe heat exchanger and has a rated heat transfer capacity of 6 kW. Cooling water is circulated by a water pump with a rated pump capacity of 0.22 kg·s^{-1}. An electrical heater, controlled by a digital regulator, is used to ensure that the water entering the condenser is at the desired temperature. The low temperature evaporator and high temperature evaporator are double-pipe heat exchangers, each with a rated heat transfer capacity is 3 kW. An

7

electrical heater, controlled by a digital regulator, is used to ensure the chilled water entering the low-temperature

and high-temperature evaporators is at the desired temperature. Chilled water is circulated by a water pump.

3.2. Test conditions and measurements

The temperature, pressure, and flow rates of the working fluids are measured at several locations, as shown in

Fig. 4. T-type chrome-nickel thermocouples are used to measure the temperature of the working fluids with an

accuracy of ± 0.1 °C. The temperature of the refrigerant is measured at the inlet and outlet of the condenser,

evaporator, and compressor. The temperature of the chilled water is measured at the inlet and outlet of the

evaporators. Cooling water temperature is measured at the inlet and outlet of the condenser. Four bourdon type

manometers are used at the inlet and outlet of the compressor and expansion valve. Turbine flow-meters are used to

measure the flow rates of the chilled water and cooling water. The compressor input power is measured by a digital

wattmeter. The working refrigerant is R32/R236fa, with W(R32) between 0.3 and 0.6.

3.3. Uncertainty of the experimental data

Some parameters, such as the temperature and pressure, are measured directly, while the other parameters, such

as the *COP*, refrigerating capacity, and the second law efficiency cannot be measured directly. The uncertainties

resulting from measuring devices and experimental fluctuations are analyzed according to the principle of

uncertainty propagation, as shown in Eqs. (8-10). The average uncertainties of the calculated parameters are shown

in Table 3,

$$y = f(x_1, x_2, ..., x_n) \tag{8}$$

$$\Delta y = \frac{\partial f}{\partial x_1} \Delta x_1 + \frac{\partial f}{\partial x_2} \Delta x_2 + \cdots + \frac{\partial f}{\partial x_n} \Delta x_n \tag{9}$$

$$\varepsilon = \frac{\Delta y}{y} = \frac{1}{y} \left(\frac{\partial f}{\partial x_1} \Delta x_1 + \frac{\partial f}{\partial x_2} \Delta x_2 + \cdots + \frac{\partial f}{\partial x_n} \Delta x_n \right) \tag{10}$$

Where Δy represents the overall uncertainty associated with independent parameter y. Variables Δx_1, Δx_2, Δx_3 ....Δx_n

8

represent the uncertainties of the measuring devices and the experimental fluctuations associated with independent parameters $x_1, x_2, x_3, \ldots, x_n$. The relative error of parameter y is denoted by ε.

3.4. Performance of experimental setup

The experimental coefficient of performance (COP_{exp}) for the proposed chiller is evaluated using the following equation:

$$COP_{\exp} = \frac{Q_{\exp}}{N_{com}} = \frac{Q_{eva,H} + Q_{eva,L}}{N_{com}} = \frac{C_P G_H \left(t_{H,in} - t_{H,out} \right) + C_P G_L \left(t_{L,in} - t_{L,out} \right)}{N_{com}} \tag{11}$$

The second law efficiency of the proposed chiller (η) is defined as the ratio between the chiller performance and the performance of the ideal Lorenz cycle (COP_{lo}).

$$\eta = \frac{COP_{\exp}}{COP_{lo}} \tag{12}$$

4. Results and discussion

4.1. System performance with varying mass fraction of R32

Fig. 5 shows the variation in theoretical performance (COP_{th}) and experimental performance (COP_{exp}), of the proposed chiller, caused by varying the mass fraction of R32 (W(R32)), with different chilled water outlet temperatures ($T_{L,out}$ and $T_{H,out}$). Both COP_{th} and COP_{exp} increase as W(R32) increases from 0.3 to 0.6; this is because the specific refrigerating capacity of R32 is larger than that of R236fa under the same working conditions. The maximum COP occurs as W(R32) is 0.6. In Fig. 5(a), the maximum COP_{th} is 4.5, while the maximum COP_{exp} is 3.87. In Fig. 5(b), the maximum COP_{th} and COP_{exp} are 4.6 and 3.92, respectively. In Fig. 5(c), the maximum COP_{th} is 17.5% larger than COP_{exp}. In Fig. 5(d), the maximum COP_{th} is 4.8, and the maximum COP_{exp} is 4.1.

4.2. Second law efficiency with varying mass fraction of R32

Fig. 6 shows the second law efficiency (η) is affected by changes in the mass fraction of R32 (W(R32)), with different chilled water outlet temperatures ($T_{L,out}$ and $T_{H,out}$). As shown, η increases significantly with the increase of W(R32); this is a result of an increasing COP_{exp} as W(R32) increases, as shown in Fig. 5, while the COP_{lo} remains

9

constant. When W(R32) increases from 0.3 to 0.6, η increases to an average of 31%. When $T_{H,out}$ is 16 °C and $T_{L,out}$ is 6 °C, the maximum and minimum η are 0.318 and 0.239, respectively. When $T_{H,out}$ is 17 °C and $T_{L,out}$ is 7 °C, the maximum and minimum η are 0.311 and 0.242, respectively. When $T_{H,out}$ is 17 °C and $T_{L,out}$ is 8 °C, the maximum η is 0.309, and the minimum η is 0.24.

4.3. System performance with varying chilled water temperature

Table 4 shows the changes in theoretical performance (COP_{th}), experimental performance (COP_{exp}), and the second law efficiency (η) of the proposed chiller, while varying the chilled water temperature and mass fraction of R32 (W(R32)). It can be seen that the proposed chiller can produce chilled water with different temperatures, where the low temperature chilled water can be at 6-8 °C, and the high temperature chilled water can be at 14-18 °C. Both COP_{exp} and COP_{th} increase with the increase of the chilled water temperature. When W(R32) is 0.3, the maximum COP_{exp} and COP_{th} are 3.18 and 4.54, respectively, while the minimum COP_{exp} and COP_{th} are 2.81 and 4.09, respectively. When W(R32) is 0.4, the maximum COP_{exp} and COP_{th} are 3.73 and 4.58, respectively, and the minimum COP_{exp} and COP_{th} are 3.41 and 4.11, respectively. As W(R32) is 0.5, the maximum COP_{exp} and COP_{th} are 3.89 and 4.7, while the minimum COP_{exp} and COP_{th} are 3.58 and 4.28 respectively. When W(R32) is 0.6, the maximum COP_{exp} and COP_{th} are 4.11 and 4.89, respectively, and the minimum COP_{exp} and COP_{th} are 3.82 and 4.46 respectively. The second law efficiency is not significantly influenced by varying the chilled water temperature. When W(R32) is 0.3, 0.4, 0.5 and 0.6, the second law efficiency is around 0.24, 0.285, 0.3, and 0.31, respectively.

4.4. System performance with varying flow rates of heat transfer media

Fig. 7 shows the change in experimental performance (COP_{exp}) while varying the flow rates of heat transfer media (chilled water and cooling water), where $T_{L,out}$=7 °C, $T_{H,outt}$=16 °C and $T_{cw,out}$=32 °C. In general, COP_{exp} increases as the cooling water flow rate (G_{cw}) increases. This is because a higher cooling water flow rate will decrease the condensing temperature when the inlet and outlet temperatures of the cooling water in the condenser

10

are held constant; this results in lower power consumption of the compressor. In addition, the increased chilled water flow rate (G_H and G_L) can improve the performance of the proposed chiller. This is due to the fact that a higher chilled water flow rate will decrease the evaporating temperature when the inlet and outlet temperatures of the chilled water in the evaporators remain constant; this leads to higher refrigerating capacity and lower power consumption of the compressor.

In Fig. 7(a), the maximum COP_{exp} is 3.97 when the flow rate of the chilled water is 0.125 kgs^{-1} and the flow rate of the cooling water is 0.22 kg s^{-1}. The minimum COP_{exp} is 3.26 when the flow rate of the chilled water is 0.069 kg s^{-1} and the flow rate of the cooling water is 0.11 kg s^{-1}. The COP_{exp} increases by 22% due to the increased flow rates of the chilled water and cooling water. In Fig. 7(b), the maximum COP_{exp} is 4.08 while the flow rate of the chilled water is 0.125 kg s^{-1} and the flow rate of the cooling water is 0.22 kg s^{-1}. The minimum COP_{exp} is 3.49 when the flow rate of the chilled water is 0.069 kg s^{-1} and the flow rate of the cooling water is 0.14 kg s^{-1}. The COP_{exp} increases by 17% on average. In Fig. 7(c), the maximum COP_{exp} is 4.17 when the flow rate of the chilled water is 0.11 kg s^{-1} and the flow rate of the cooling water is 0.22 kg s^{-1}. The minimum COP_{exp} is 3.73 when the flow rate of the chilled water flow rate is 0.069 kg s^{-1} and the flow rate of the cooling water is 0.167 kg s^{-1}. The COP_{exp} increases by an average of 12%.

5. Conclusions

In this paper, a novel double temperature chiller is proposed, with the zeotropic refrigerant R32/R236fa.This chiller can produce high temperature chilled water (around 16 °C) and low temperature chilled water (around 7 °C) simultaneously, which can be applied in the temperature and humidity independent control system. Changes in the system's theoretical performance (COP_{th}), experimental performance (COP_{exp}) and the second law efficiency (η) are studied as functions of the mass fraction of R32 in refrigerant mixture R32/R236fa (W(R32)), temperature of the chilled water, and flow rates of heat transfer media (chilled water and cooling water). The main results are shown as

11

follows:

(1) COP_{exp}, COP_{th}, and the second law efficiency η increase with the increase of W(R32). When W(R32) increases from 0.3 to 0.6, COP_{th} increases from 4.35 to 4.73, COP_{exp} rises from 3.08 to 3.97, and η increases to 31%.

(2) The chilled water temperature has a significant effect on COP_{exp} and COP_{th}. When W(R32) is 0.5, an increase in the chilled water temperature causes COP_{exp} to increase from 3.58 to 3.89 while COP_{th} rises from 4.28 to 4.7. The chilled water temperature has little effect on the second law efficiency η. When W(R32) is 0.3, 0.4, 0.5 and 0.6, η is 0.24, 0.285, 0.3, and 0.31, respectively.

(3) COP_{exp} increases significantly with the increased flow rates of chilled water and cooling water. When W(R32) is 0.4, COP_{exp} increases by 22%. When W(R32) is 0.5 and 0.6, COP_{exp} increases by 17% and 12%, respectively.

Acknowledgments

References

Cai, W.G., Wu, Y., Zhong, Y., Ren, H., 2009. China building energy consumption: situation, challenges and corresponding measures. Energy Policy. 37(6), 2054-2059.

Ge T.S., Dai Y.J., Wang R.Z.,2011. Performance study of silica gel coated fin-tube heat exchanger cooling system based on a developed mathematical model. Energy Conversion and Management. 52(6), 2329-2338.

Jiang Y., 2005. Current building energy consumption in China and effective energy efficiency measures. HV&AC. 35(5), 30-40.

Jung D.S., 1991. Performance simulation of a two-evaporator refrigerator-freezer charged with pure and mixed refrigerants. International Journal of Refrigeration. 14(91), 254-263.

12

Kessling W., Laevemann E., Kapfhammer C., 1998. Energy storage for desiccant cooling systems component development. Solar Energy. 64(4), 209-221.

Liu X.H., Jiang Y., Zhang T., 2013. Temperature and humidity independent control (THIC) of air-conditioning system. Springer Berlin.

Lorenz, A., Meutzner, K., 1975.Onapplicationofnon-azeotropictwocomponent refrigerants in domestic refrigerators and home freezers. XIV Int. Congress Refrigeration, Moscow. IIR, Paris.

Lowenstein A., Slayzak S., Kozubal E., 2006. A zero carryover liquid-desiccant air conditioner for solar applications. ASME 2006 International Solar Energy Conference. American Society of Mechanical Engineers. 397-407.

Waugaman D.G., Kini A., Kettleborough C.F., 1993. A Review of Desiccant Cooling Systems. Journal of Energy Resources Technology. 115(1),1-8.

Wang Z.B., Zhang X.Y., 2013. Research of temperature and humidity independent control air-conditioning system. Advanced Materials Research. 805, 557-561.

Yang K., Yao Y., Liu S., 2012. Effect of applying ultrasonic on the regeneration of silica gel under different air conditions. International Journal of Thermal Sciences. 61(61), 67-78.

Yoon W.J., Seo K., Chung H.J., 2012. Performance optimization of a Lorenz–Meutzner cycle charged with hydrocarbon mixtures for a domestic refrigerator-freezer. International Journal of Refrigeration. 35(1), 36-46.

Zerwekh J.E., Sakhaee K., Glass K., 2012. Performance optimization of dual-loop cycles using R-600a and hydrocarbon mixtures designed for a domestic refrigerator-freezer. International Journal of Refrigeration. 35(6), 1657-1667.

Zhang, H., 2011. Performance comparison between temperature and humidity independent control and conventional air conditioning systems. Heating Ventilating and Air Conditioning. 41(1), 48-52.

13

Zhao K., Liu X.H., Zhang T., 2011. Performance of temperature and humidity independent control air-conditioning

system in an office building. Energy and Buildings. 43(8), 1895-1903.

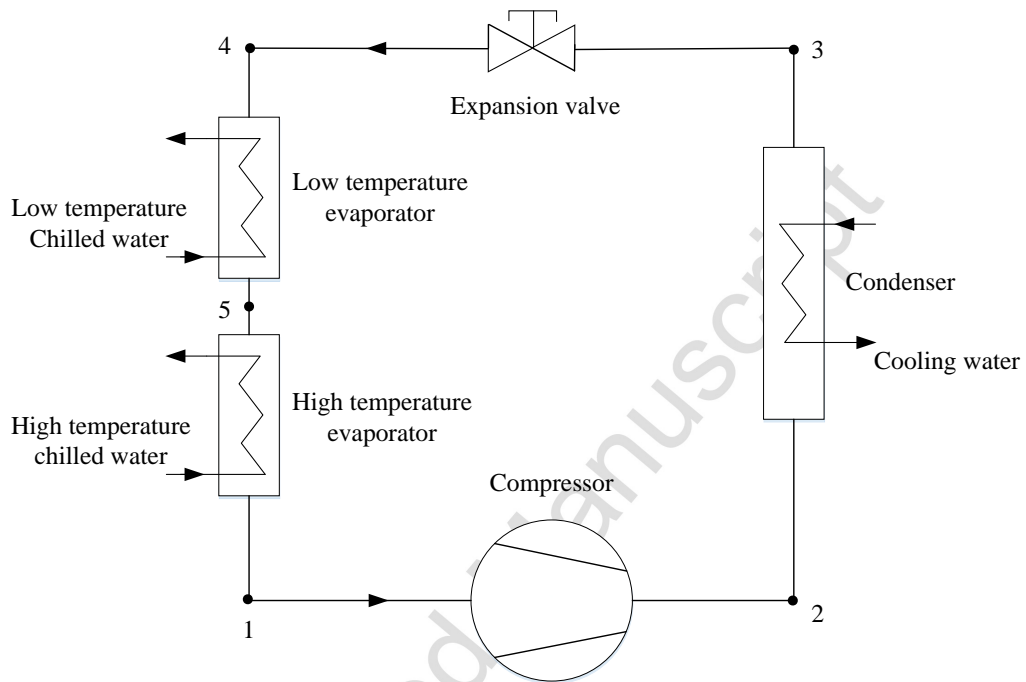Zhao R.Y., Fan C.Y., Xue D.H., Qian Y.M., 1994. Air conditioning. Architecture & Building Press, Beijing: China.

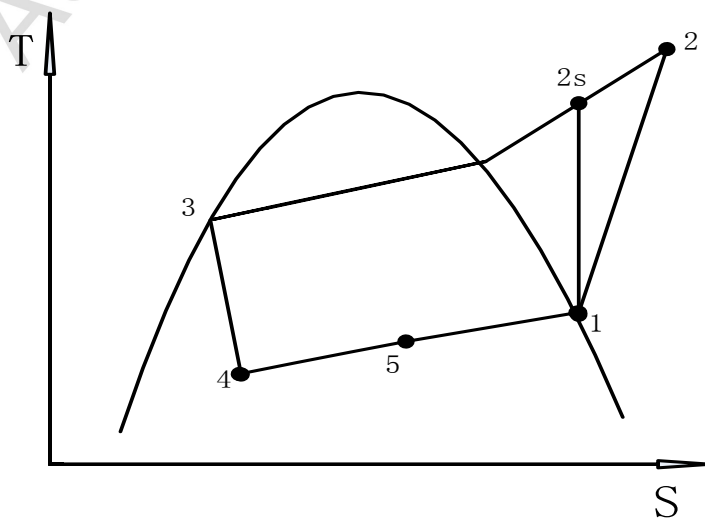**Fig. 1** Schematic of the theoretical cycle.
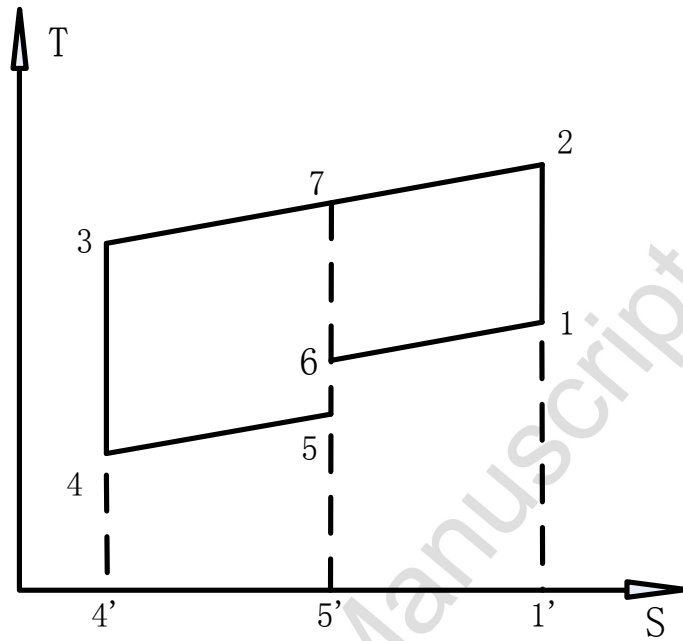

14

Fig. 2 T-S chart of the theoretical cycle.

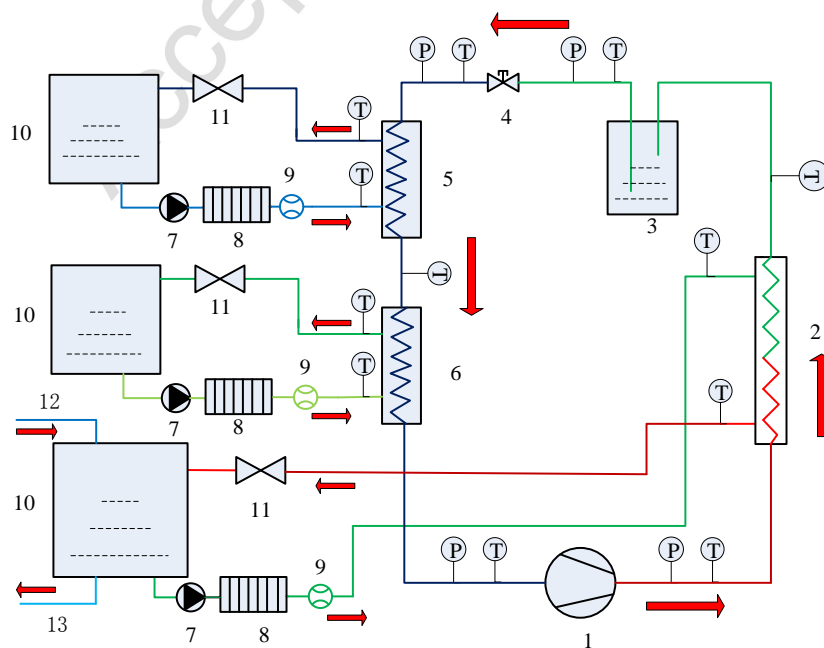**Fig. 3** The ideal Lorenz cycle with temperature glide based on the proposed chiller.

15

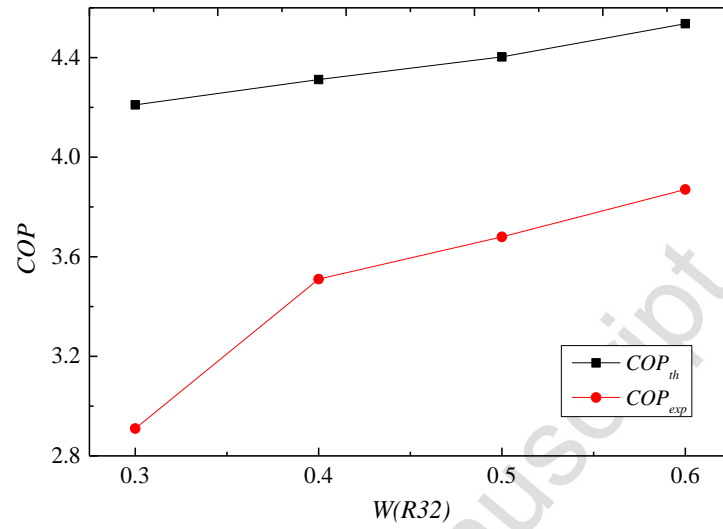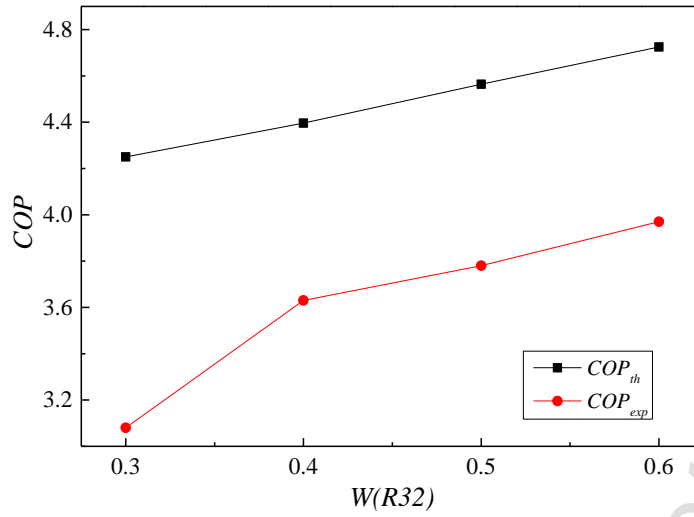**Fig. 4** Schematic of the experimental setup.

(a) $T_{L,out}$=6 °C, $T_{H,out}$=16 °C
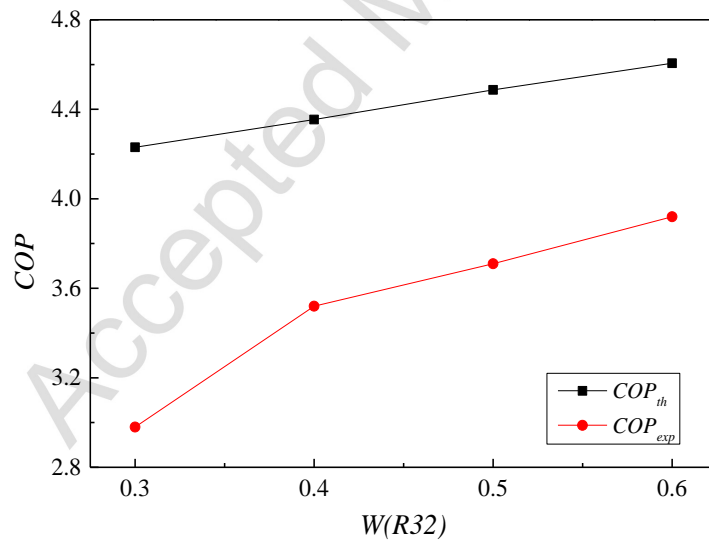
(b) $T_{L,out}$=7 °C, $T_{H,out}$=16 °C

16

(c) $T_{L,out}$=7 °C, $T_{H,out}$=17 °C
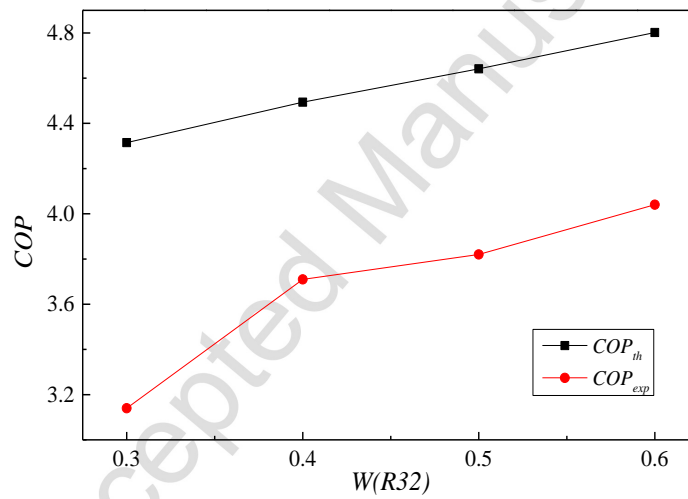
(d) $T_{L,out}$=8 °C, $T_{H,out}$=17 °C

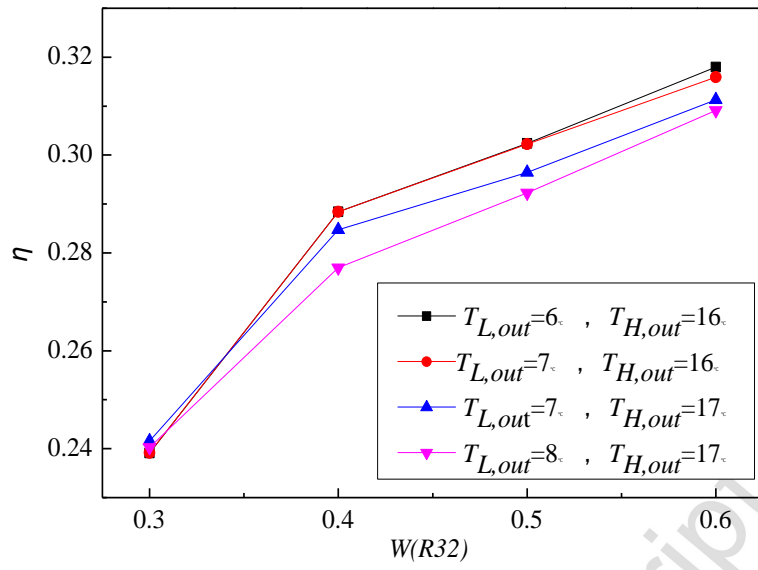**Fig. 5** Changes in *COP* due to varying the mass fraction of R32.

17

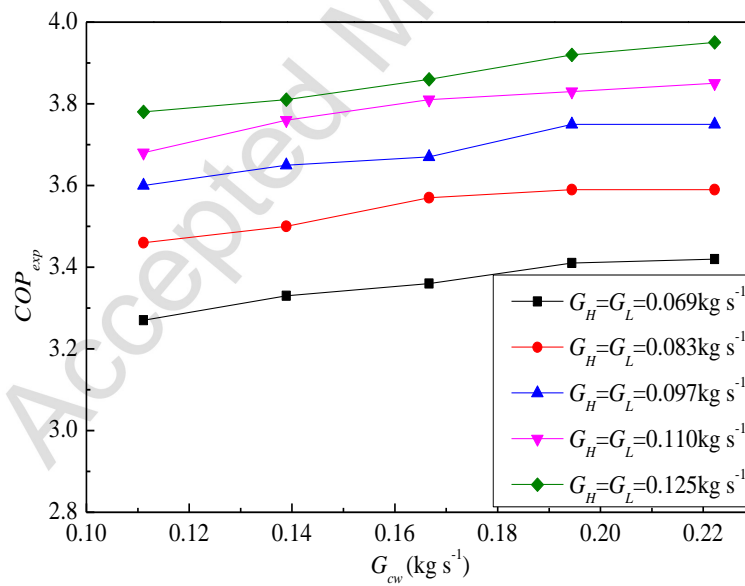**Fig. 6** Changes in the second law efficiency due to varying the mass fraction of R32.
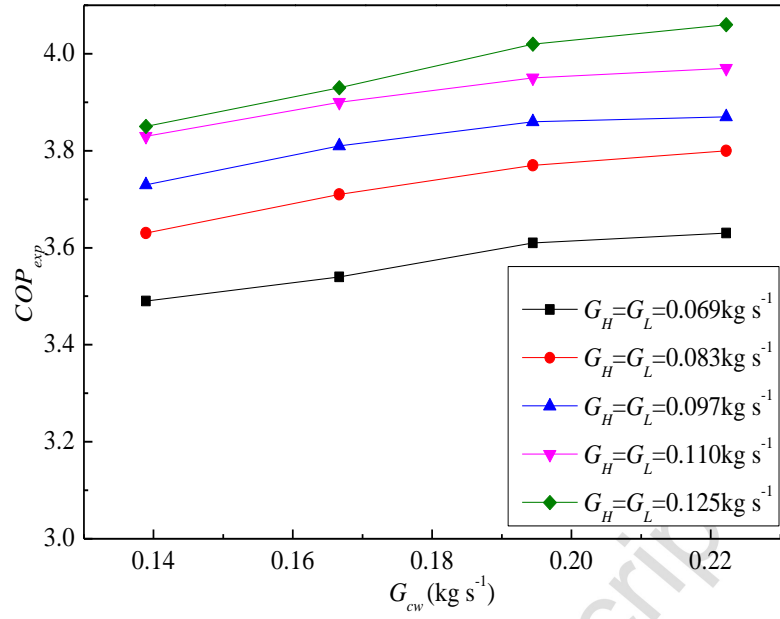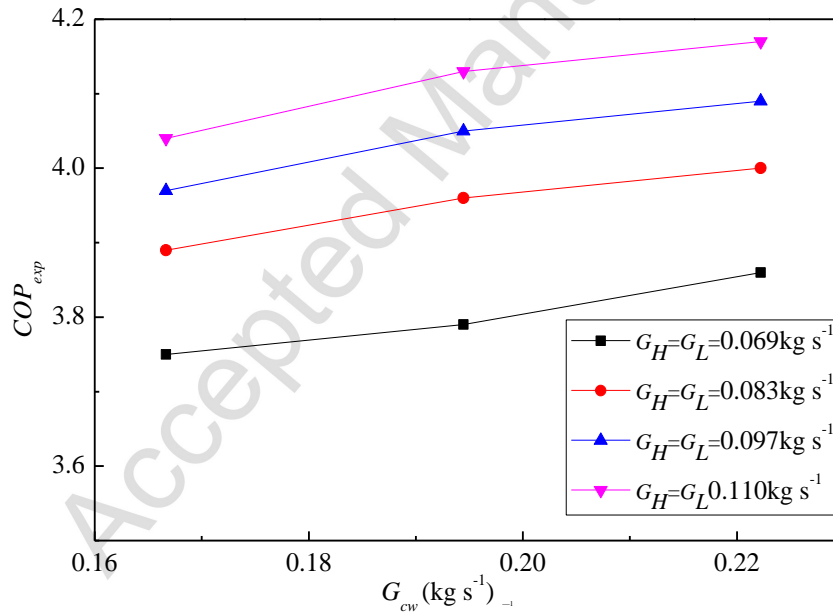

(a) W(R32)=0.4

18

(b) W(R32)=0.5

(c) W(R32)=0.6

Fig. 7 Changes in COP due to varying the flow rates of chilled water and cooling water.

19

Table 1 Basic properties of R32 and R236fa.

Refrigerant	Molecular formula	Molar mass (kg kmol^{-1})	*NBP* (°C)	T_c (°C)	P_c (MPa)	*ODP*	*GWP*
R32	CH_2F_2	152.04	-50.7	78.1	5.8	0	675
R236fa	$CF_3CH_2CF_3$	52.2	-1.44	124.9	3.2	0	6300

Table2 Thermodynamic properties of R32/R236fa at different mass fractions of R32.

W(R32)	0.3	0.4	0.5	0.6
Evaporating pressure(MPa)	0.45	0.52	0.6	0.64
T_b(°C)	-1.9	-1.7	-1.6	-1.1
T_d (°C)	19.5	17.9	15.7	13.4
Temperature glide (°C)	21.4	19.6	17.3	14.5
P_c (MPa)	4.7	5.0	5.2	5.4
T_c (°C)	104.1	99.2	94.7	90.8
Molar mass(kg kmol^{-1})	96.4	85.9	77.5	70.6
Latent heat capacity(kJkg^{-1})	219.29	233.92	248.37	262.26
ODP	0	0	0	0
GWP	4612	4050	3850	2925

Table 3 Uncertainty of calculated values.

20

Calculated variable	Uncertainty (%)
Coefficient of performance	10.56
Refrigerating capacity	9.56
Second law efficiency	10.56

Table 4 Changes in *COP* and second law efficiency with varying chilled water temperature and W(R32).

W(R32)	$T_{H,out}$	$T_{L,out}$	$T_{H,in}$	$T_{L,in}$	COP_{exp}	η	COP_{th}
	14.0	6.0	19.2	10.6	2.81	0.236	4.09
	15.1	6.2	20.8	10.7	2.91	0.239	4.19
0.3	16.1	7.1	21.8	11.8	2.98	0.239	4.28
	17.0	7.3	23.1	11.8	3.08	0.242	4.35
	17.2	8.1	23.1	13.0	3.14	0.240	4.45
	17.9	8.2	24.2	12.9	3.18	0.237	4.54
	14.9	6.0	19.7	10.5	3.41	0.287	4.11
	16.0	6.1	21.2	10.5	3.51	0.288	4.31
	17.1	6.1	22.7	10.2	3.60	0.289	4.35
	15.9	7.0	20.6	11.8	3.52	0.283	4.35
0.4	17.0	7.1	22.2	11.7	3.63	0.285	4.40
	18.0	7.1	23.8	11.3	3.71	0.284	4.49
	15.9	8.0	20.3	13.2	3.56	0.279	4.40
	17.0	8.0	21.8	12.9	3.62	0.277	4.49
	18.0	8.0	23.2	12.9	3.73	0.279	4.58
0.5	15.0	6.0	19.6	11.4	3.58	0.301	4.28

21

	16.2	6.2	21.4		3.68	0.302	4.40
	17.0	5.9	22.8	10.7	3.76	0.302	4.49
	16.0	7.1	20.7	12.8	3.71	0.298	4.49
	17.0	7.1	22.2	12.5	3.78	0.296	4.56
	18.1	7.0	23.8	12.2	3.87	0.297	4.64
	16.1	7.9	20.3	14.2	3.77	0.295	4.56
	17.1	8.0	21.8	14.0	3.82	0.292	4.64
	18.2	8.1	23.3	13.9	3.89	0.291	4.70
	14.9	5.8	19.7	11.1	3.82	0.321	4.46
	15.9	6.1	21.1	11.3	3.87	0.318	4.54
	16.9	5.9	22.5	10.8	3.93	0.316	4.61
0.6	16.1	6.9	20.8	12.5	3.92	0.315	4.61
	16.9	6.9	22.1	12.1	3.97	0.311	4.73
	17.1	7.9	21.8	13.9	4.04	0.309	4.80
	18.0	8.1	23.0	13.9	4.11	0.307	4.89

22